

ACA-24-2529 Rev.Highlighted

ELECTRONIC SUPPLEMENTARY INFORMATION

Characterization of Monoclonal Antibody Charge Variants under Near-Native Separation Conditions using Nanoflow Sheath Liquid Capillary Electrophoresis-Mass Spectrometry

Annika A.M. van der Zon^{1,2,*}, Alisa Höchsmann^{3,4}, Tijmen S. Bos^{1,2}, Christian Neusüß³, Govert W. Somsen^{2,5}, Kevin Jooß^{2,5,*}, Rob Haselberg^{2,5,*} and Andrea F.G. Gargano^{1,2,*}

¹ University of Amsterdam, van 't Hoff Institute for Molecular Sciences, Analytical Chemistry Group, Science Park 904, 1098 XH Amsterdam, The Netherlands

² Centre of Analytical Sciences Amsterdam, Science Park 904, 1098 XH Amsterdam, The Netherlands

³ Aalen University, Department of Chemistry, Beethovenstraße 1, 73430 Aalen, Germany

⁴ Eberhard Karls University of Tübingen, Faculty of Science, 72074 Tübingen, Germany

⁵ Vrije Universiteit Amsterdam, Department of Chemistry and Pharmaceutical Sciences, Amsterdam Institute of Molecular and Life Sciences, Division of BioAnalytical Chemistry, De Boelelaan 1085, 1081 HV Amsterdam, The Netherlands

* Correspondence: a.a.m.vanderzon@uva.nl, k.jooss@vu.nl, rob.haselberg@vectorytx.com, and a.gargano@uva.nl

Contents

S-I NanoCEasy interface _____	3
S-II Information mAbs _____	4
S-III EOF suppression by HPMC coating _____	5
S-V Effect of protein concentration on the separation of mAbs _____	10
S-VI Comparison with established EACA-based CZE-UV method _____	12
S-VII Optimization CZE-MS method _____	14
S-VIII Profiling of mAbs by CZE-MS _____	19
References _____	24

S-I NanoCEasy interface

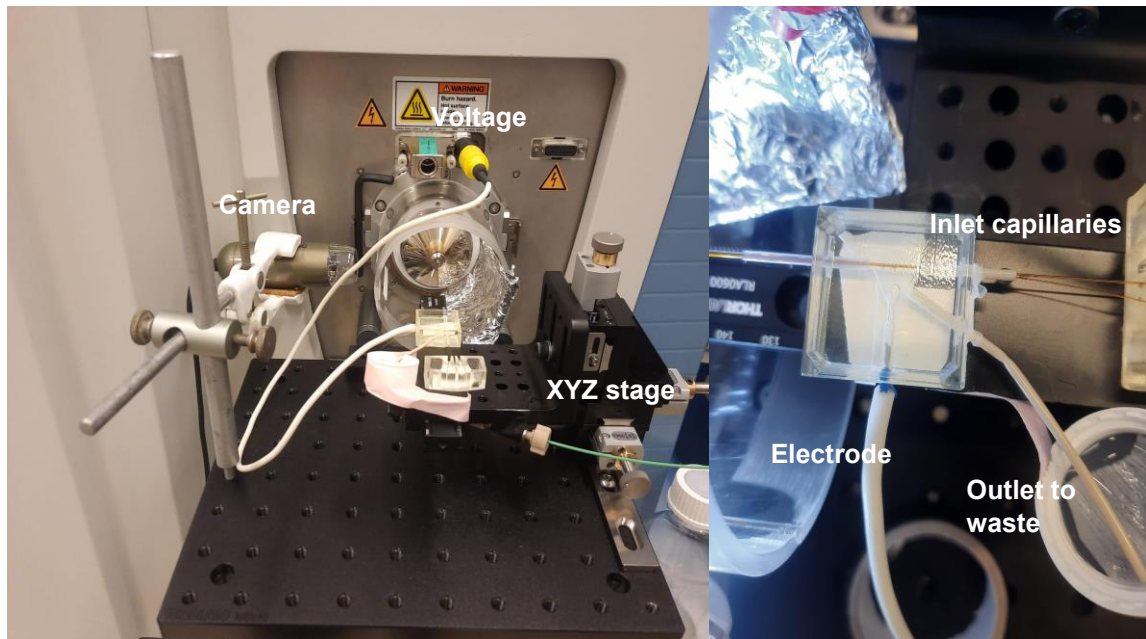


Fig. S1: Configuration of the nanoCEasy interface

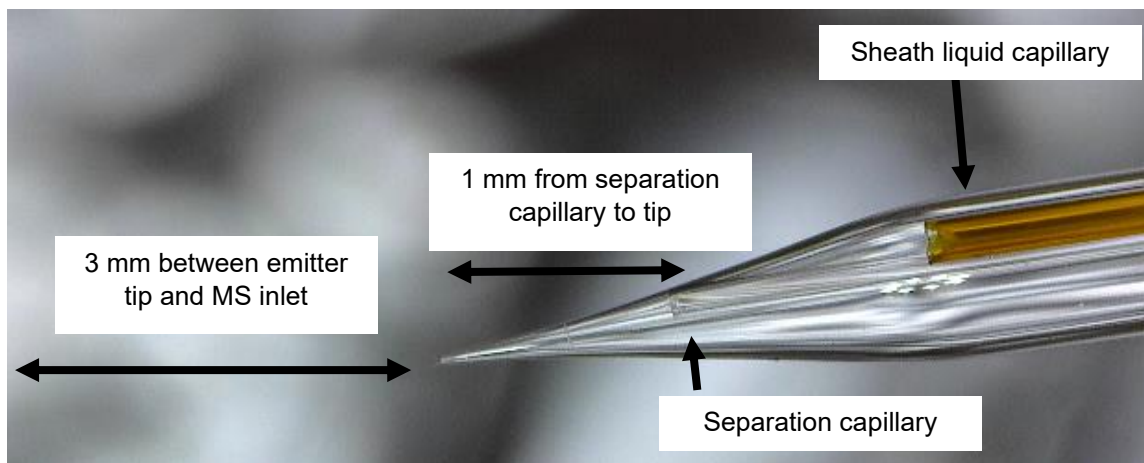


Fig. S2: Emitter of the nanoCEasy interface (separation mode)

S-II Information mAbs

Table S1: Information regarding (i) IgG subclass, (ii) isoelectric point (pI), and (iii) post-translational modifications (PTMs) of the four commercially available mAbs used in this study.

Name mAb	IgG subclass	pI	PTMs	Ref.
Rituximab	IgG ₁	9.1-9.4	N-terminal pyroglutamate (2 x light chain, 2 x heavy chain), incomplete C-terminal lysine clipping, N-glycosylation, sialylation, deamidation	[1,2]
NISTmAb	IgG ₁	8.8-9.2	Deamidation, incomplete C-terminal lysine variants, N-terminal pyroglutamate (2 x heavy chain), glycation, N-glycosylation	[1,3]
Cetuximab	IgG ₁	8.7-8.9	N-terminal pyroglutamate (2 x heavy chain), N-glycosylation, sialylation, incomplete C-terminal lysine clipping	[1,4]
Pembrolizumab	IgG ₄	7.4-7.8	N-terminal pyroglutamate (2 x heavy chain), N-glycosylation, incomplete C-terminal lysine clipping, deamidation, Des-GK truncation	[1,5,6]

S-III EOF suppression by HPMC coating

Electroosmotic flow

The EOF of HPMC-coated capillaries was determined by analyzing 20 mM acrylamide using +30 kV while applying different pressures (10-100 mbar) during the measurement. The reciprocal migration time of acrylamide (EOF marker) is plotted against the applied pressures in Fig. S3. The reciprocal EOF time is found by extrapolating the linear curve to zero applied pressure. The negative power of the intercept results in the migration time of the EOF when no pressure is applied. With this, the EOF mobility could be calculated (Eq. S2). At pH 5.0 and 2.8, the μ_{eof} is $7.06 \cdot 10^{-10} \text{ m}^2\text{v}^{-1}\text{s}^{-1}$ (RSD=3.7%, n=3) and $7.52 \cdot 10^{-10} \text{ m}^2\text{v}^{-1}\text{s}^{-1}$ (RSD=6.4%, n=3), respectively.

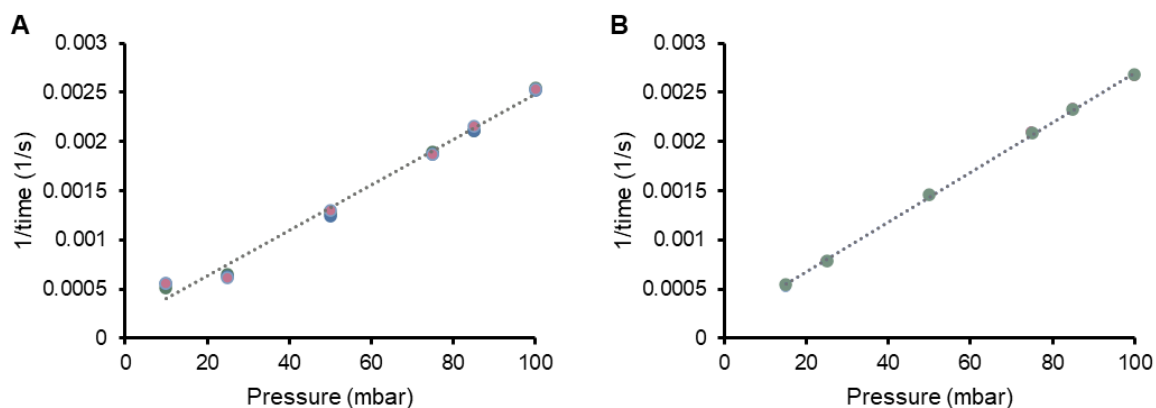


Fig. S3: Determination of EOF of HPMC-coated capillary using constant voltage and several applied pressures (10-100 mbar) for a BGE of 50 mM acetic acid adjusted to **(A)** pH 5.0 and **(B)** pH 2.8. The measurements were done in triplicate and lines were fitted by linear regression: (A) $y=2.31 \cdot 10^{-5}x + 1.71 \cdot 10^{-4}$ ($R^2=0.9911$) and (B) $y=2.53 \cdot 10^{-5}x + 1.74 \cdot 10^{-4}$ ($R^2=0.9996$). Conditions: HPMC coated capillary (50 μm x 60 cm) and applied voltage +30 kV.

Repeatability

The repeatability of the selected CZE-UV method (BGE of 50 mM acetic acid (pH 2.8 and 5.0) at +25 kV) was assessed. Pembrolizumab was analyzed five times on two consecutive days (Fig. S4). The RSD of the migration time of the main isoform within one day (n=5) was 0.3%. The repeatability (RSD) over two days (n=10), an RSD was 2.1%. The in-between repeatability of the HPMC-coated capillaries was also tested by analyzing pembrolizumab (n=5 per capillary) with three separately coated HPMC capillaries. The RSD of the migration time of pembrolizumab was 0.11%, indicating low variance between distinct HPMC capillaries. In addition, at least 40 runs could be executed on a single HPMC capillary without loss of separation performance and migration time stability (data not shown).

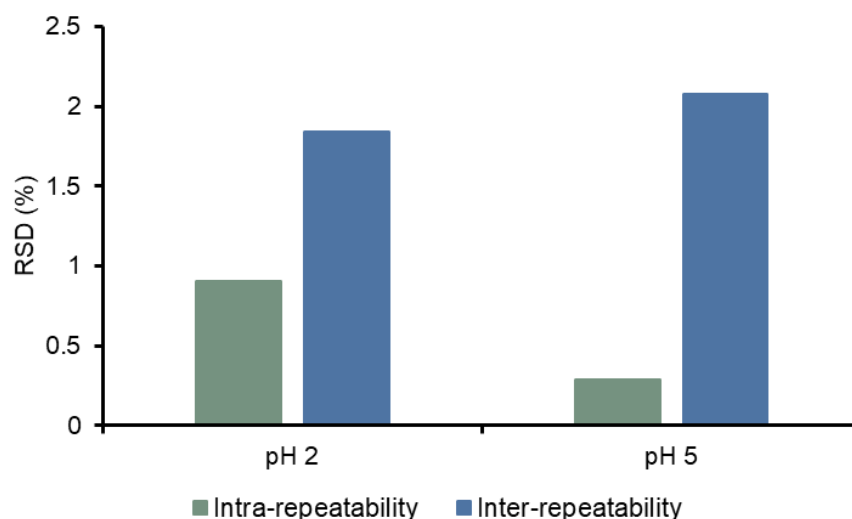


Fig. S4: RSD values for migration time of main isoform of pembrolizumab determined on one day (n=5) and two days (n=10). Conditions: HPMC coated capillary (50 μm x 60 cm), BGE: 50 mM acetic acid (pH 2.8 or pH 5.0), separation voltage +25 kV, 1 $\text{mg}\cdot\text{mL}^{-1}$ pembrolizumab injected.

S-IV CZE method development and evaluation

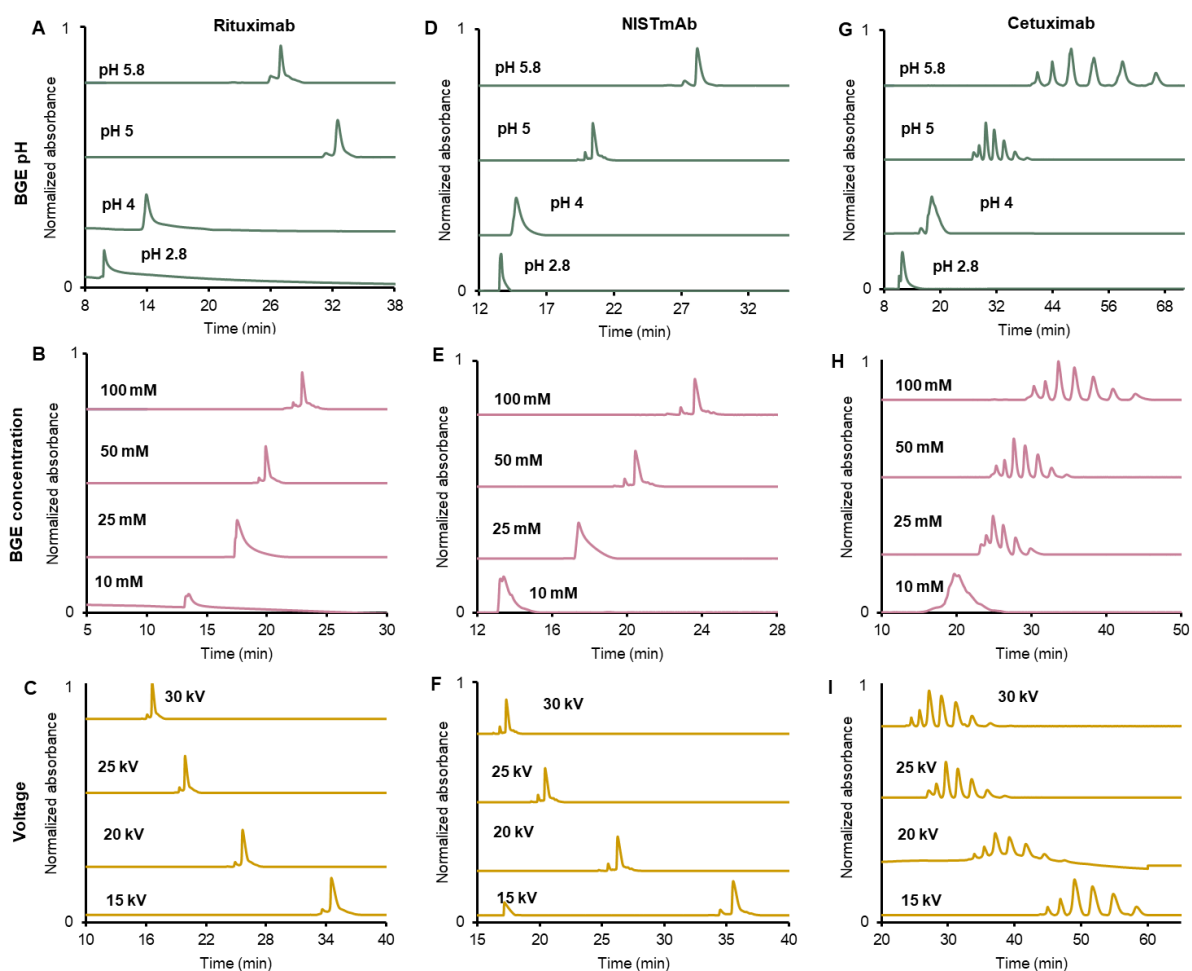


Fig. S5: CZE-UV analysis of rituximab, NISTmAb, and cetuximab ($1.0 \text{ mg}\cdot\text{mL}^{-1}$) using **(A,D,G)** BGEs of 50 mM acetic acid adjusted to various pH values (2.8, 4.0, 5.0 and 5.8), **(B,E,H)** BGE at various acetic acid concentrations (10-100 mM) adjusted to pH 5.0, and **(C,F,I)** a BGE of 50 mM acetic acid (pH 5.0) applying various voltages (+15-30 kV). Conditions: HPMC-coated capillary ($50 \mu\text{m}$ i.d. x 60 cm) and separation voltage +25 kV (A and B). See section 2.4.1 for additional CE conditions. At a higher pH, the mobility of the mAbs is lower, resulting in a better variant separation. This is also true when using a higher BGE concentration. However, the addition of ammonium hydroxide to the BGE for pH adjustment causes an increase in CE current for the less acidic BGEs, which is not ideal for CZE-MS. The CE current can be reduced by applying a somewhat lower voltage as the separation is preserved.

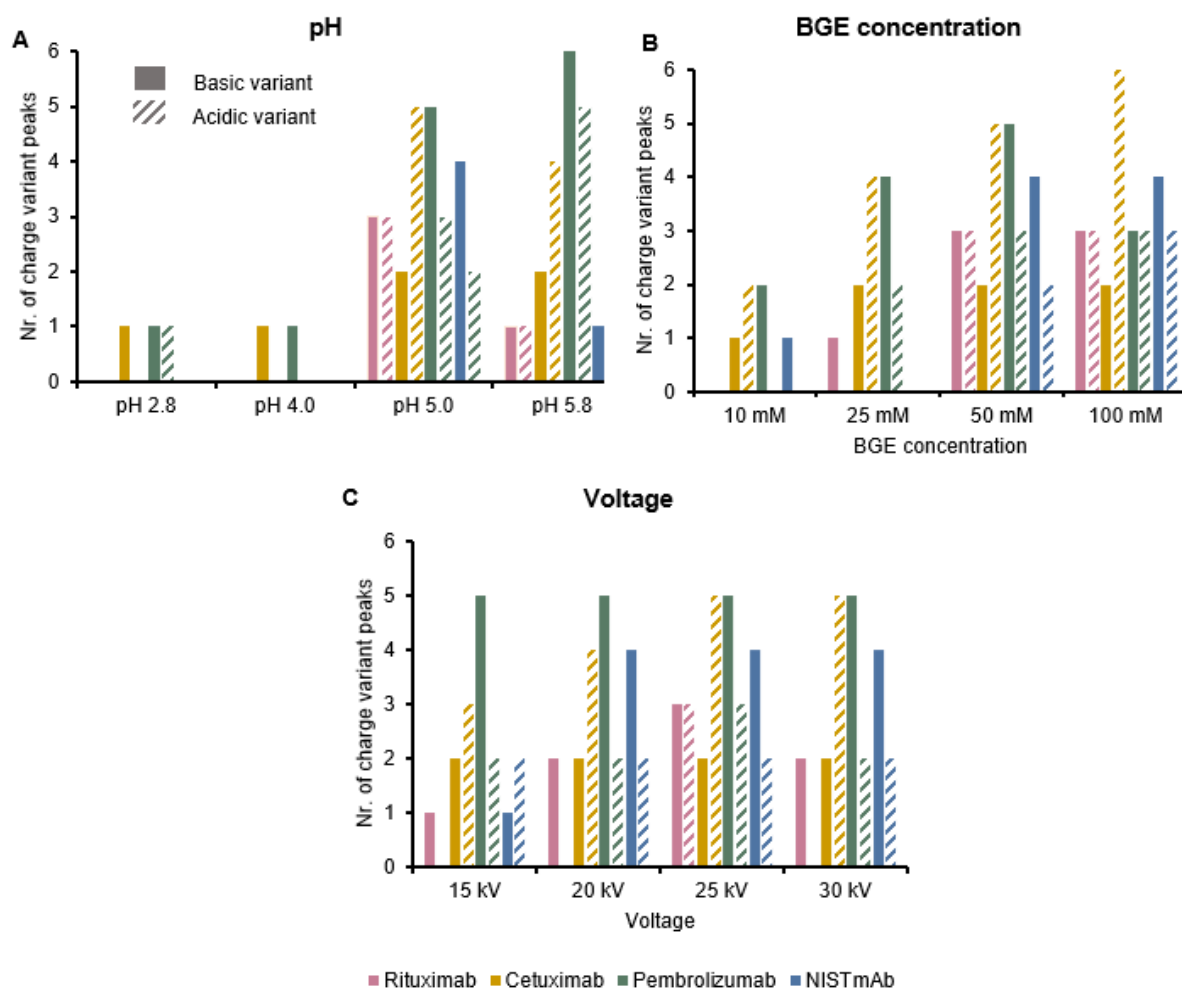


Fig. S6: The number of charge variant peaks (acidic variants (dashed) and basic variants (solid)) that were observed during optimization of various CZE-UV parameters (Fig. S5): **(A)** BGEs of 50 mM acetic acid adjusted to various pH values (2.8, 4.0, 5.0 and 5.8), **(B)** BGE at various acetic acid concentrations (10-100 mM) adjusted to pH 5.0, and **(C)** a BGE of 50 mM acetic acid (pH 5.0) applying various voltages (+15-30 kV). Conditions: HPMC-coated capillary (50 μm i.d. x 60 cm) and separation voltage +25 kV (A and B). See section 2.4.1 for additional CE conditions. Four antibodies were analyzed: rituximab (pink), cetuximab (yellow), pembrolizumab (green), and NISTmAb (blue). Conditions: HPMC-coated capillary (50 μm i.d. x 60 cm) and separation voltage +25 kV (A and B). See section 2.4.1 for additional CE conditions.

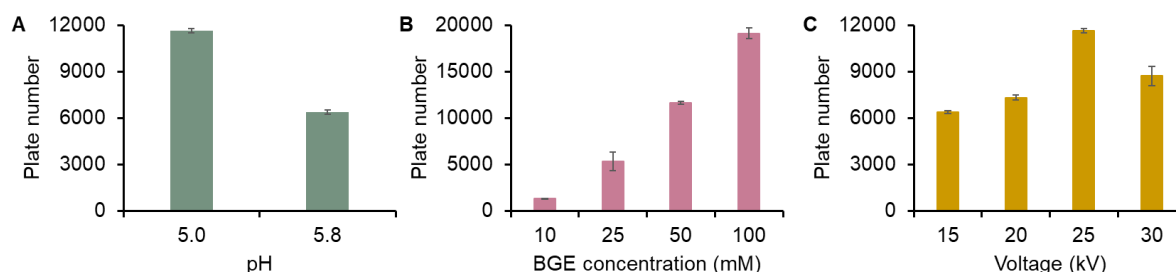


Fig. S7: Plate numbers ($n=3$) calculated (Eq. S1) of main isoform of pembrolizumab (1.0 $\text{mg}\cdot\text{mL}^{-1}$) obtained by CZE-UV using **(A)** BGEs of 50 mM acetic acid adjusted to various pH values (5.0-5.8), **(B)** BGE at various acetic acid concentrations (10-100 mM) adjusted to pH 5.0, and **(C)** a BGE of 50 mM acetic acid adjusted to pH 5.0 applying various voltages (+15-30 kV). Conditions: HPMC-coated capillary (50 μm i.d. x 60 cm), separation voltage +25 kV (A and B). See section 2.4.1 for other CE conditions.

The plate numbers and electrophoretic mobility of the main isoform of pembrolizumab obtained with CZE-MS were calculated by using Equations S1-S3.

Eq. S1: Plate number [7]

$$N = 5.54 \cdot \left(\frac{t}{W_{0.5}} \right)^2$$

Where N is the plate number, t is the migration time and $W_{0.5}$ is the peak width at half height of the peak.

Eq. S2: Apparent electrophoretic mobility [8]

$$\mu_a = \frac{L_d \cdot L}{t \cdot V}$$

Where the apparent electrophoretic mobility is μ_a , L_d is the capillary length to the detector, L is the total length of the capillary, t is the migration time and V is the applied voltage

Eq. S3: Effective electrophoretic mobility

$$\mu_e = \mu_a - \mu_{EOF}$$

Where the effective electrophoretic mobility is the difference between the apparent electrophoretic mobility (μ_a) and the electroosmotic flow (μ_{EOF}).

Table S2: The number of resolved peaks (including main isoform, basic, and acidic variants), full width at half maximum (FWHM), apparent electrophoretic mobility (μ_a), effective electrophoretic mobility (μ_e), and plate number (N) of main isoform obtained during CZE-UV of pembrolizumab ($1 \text{ mg} \cdot \text{mL}^{-1}$) using various pH and concentration of the BGE and applied voltages. Conditions: 50 mM acetic acid (unless stated otherwise) adjusted to pH 5.0 (unless stated otherwise) with ammonium hydroxide and +25 kV applied voltage (unless stated otherwise).

	N° resolved peaks	FWHM (min); RSD (%)	μ_a ($\text{m}^2 \cdot \text{V}^{-1} \cdot \text{s}^{-1}$); RSD (%)	μ_e ($\text{m}^2 \cdot \text{V}^{-1} \cdot \text{s}^{-1}$); RSD (%)	N; RSD (%)
<i>pH of BGE</i>					
2.8	2	0.51 (RSD=2.85)	$1.72 \cdot 10^{-8}$ (RSD=1.86)	$1.64 \cdot 10^{-8}$ (RSD=1.94)	3179.01 (RSD=2.91)
4.0	1	0.75 (RSD=3.01)	$1.23 \cdot 10^{-8}$ (RSD=0.58)	$1.16 \cdot 10^{-8}$ (RSD=0.62)	2767.19 (RSD=4.95)
5.0	9	0.68 (RSD=0.39)	$6.62 \cdot 10^{-9}$ (RSD=0.28)	$5.91 \cdot 10^{-9}$ (RSD=0.31)	11650.84 (RSD=1.23)
5.8	12	1.82 (RSD=2.03)	$3.34 \cdot 10^{-9}$ (RSD=1.12)	$2.63 \cdot 10^{-9}$ (RSD=1.43)	6396.95 (RSD=2.02)
<i>BGE concentration (mM)</i>					
10	3	1.23 (RSD=1.27)	$1.12 \cdot 10^{-8}$ (RSD=1.13)	$1.02 \cdot 10^{-8}$ (RSD=1.21)	1311.78 (RSD=4.72)
25	7	0.94 (RSD=8.17)	$7.09 \cdot 10^{-9}$ (RSD=1.27)	$6.38 \cdot 10^{-9}$ (RSD=1.41)	5357.73 (RSD=18.92)
50	9	0.68 (RSD=0.39)	$6.62 \cdot 10^{-9}$ (RSD=0.28)	$5.91 \cdot 10^{-9}$ (RSD=0.31)	11650.84 (RSD=1.23)
100	7	0.63 (RSD=0.64)	$5.53 \cdot 10^{-9}$ (RSD=0.88)	$4.91 \cdot 10^{-9}$ (RSD=1.02)	19144.64 (RSD=2.99)
<i>Voltage (kV)</i>					
15	8	1.68 (RSD=1.02)	$3.62 \cdot 10^{-9}$ (RSD=1.38)	$2.91 \cdot 10^{-9}$ (RSD=1.71)	6369.34 (RSD=1.46)
20	8	1.17 (RSD=0.65)	$4.86 \cdot 10^{-9}$ (RSD=0.46)	$4.15 \cdot 10^{-9}$ (RSD=0.53)	7330.833 (RSD=2.12)
25	9	0.68 (RSD=0.39)	$6.62 \cdot 10^{-9}$ (RSD=0.28)	$5.91 \cdot 10^{-9}$ (RSD=0.31)	11650.84 (RSD=1.23)
30	8	0.67 (RSD=3.51)	$7.79 \cdot 10^{-9}$ (RSD=0.37)	$7.09 \cdot 10^{-9}$ (RSD=0.41)	8724.35 (RSD=7.17)

S-V Effect of protein concentration on the separation of mAbs

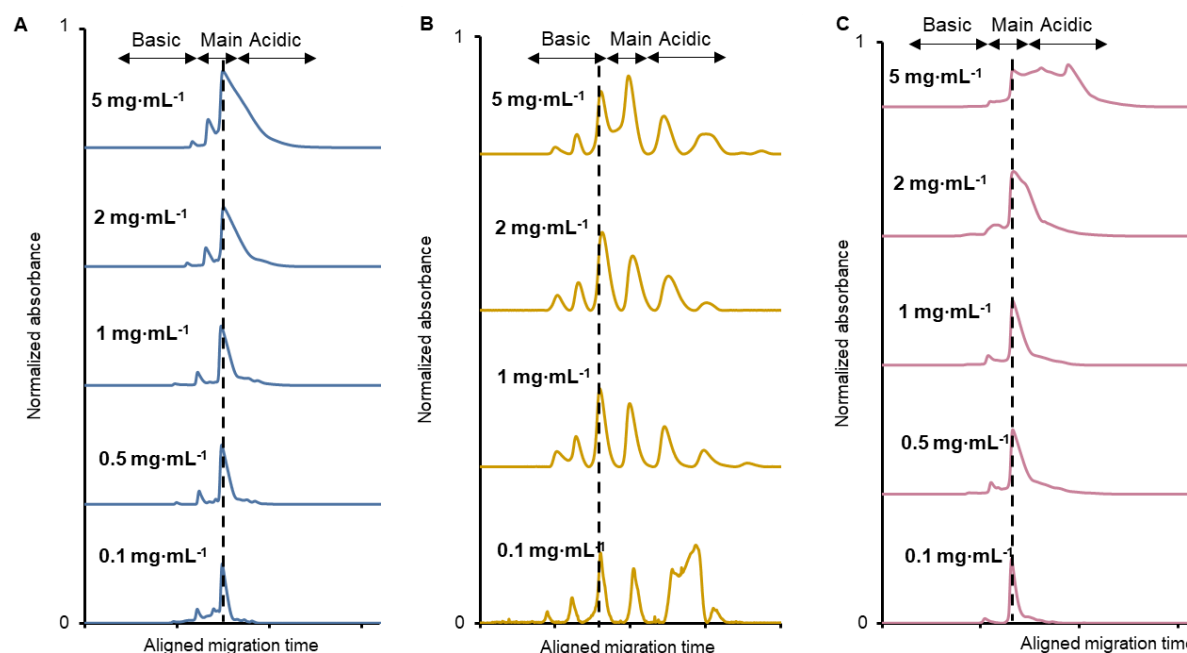


Fig. S8: CZE-UV of (A) NISTmAb (blue), (B) cetuximab (yellow), and (C) rituximab (pink) at various injected mAb concentrations ($0.1 \text{ mg}\cdot\text{mL}^{-1}$, $0.5 \text{ mg}\cdot\text{mL}^{-1}$, $1 \text{ mg}\cdot\text{mL}^{-1}$, $2 \text{ mg}\cdot\text{mL}^{-1}$, and $5 \text{ mg}\cdot\text{mL}^{-1}$). The migration times of the peaks are aligned based on the top of the peak of the main isoform (black dot line). Conditions: HPMC-coated capillary ($50 \mu\text{m}$ i.d. x 60 cm), BGE 50 mM acetic acid (pH 5.0), separation voltage $+25 \text{ kV}$. See section 2.4.1 for additional CE conditions

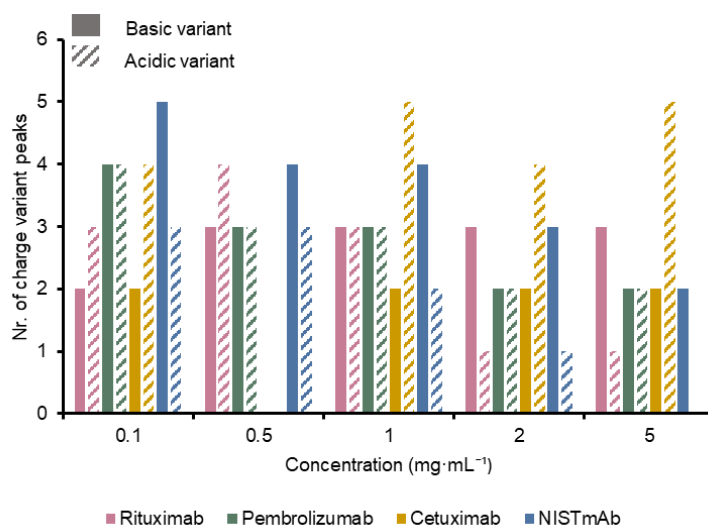


Fig. S9: The number of charge variant peaks (acidic variants (dashed) and basic variants (solid)) determined by CZE-UV (Fig. S8) using various concentrations ($0.1 \text{ mg}\cdot\text{mL}^{-1}$, $0.5 \text{ mg}\cdot\text{mL}^{-1}$, $1 \text{ mg}\cdot\text{mL}^{-1}$, $2 \text{ mg}\cdot\text{mL}^{-1}$, $5 \text{ mg}\cdot\text{mL}^{-1}$). Four antibodies were analyzed: rituximab (pink), cetuximab (yellow), pembrolizumab (green), and NISTmAb (blue). The numbers are based on triplicate measurements. Conditions: HPMC-coated capillary ($50 \mu\text{m}$ i.d. x 60 cm), BGE 50 mM acetic acid (pH 5.0), separation voltage $+25 \text{ kV}$.

Table S3: The number of resolved peaks (including main isoform, basic, and acidic variants), full width at half maximum (FWHM), apparent mobility (μ_a), effective mobility (μ_e), and plate number (N) of main isoform obtained during CZE-UV of pembrolizumab at various mAb concentrations (0.1 mg·mL⁻¹, 0.5 mg·mL⁻¹, 1 mg·mL⁻¹, 2 mg·mL⁻¹, 5 mg·mL⁻¹). Conditions: HPMC-coated capillary (50 μ m i.d. x 60 cm), BGE 50 mM acetic acid (pH 5.0), separation voltage +25 kV.

Concentration (mg·mL ⁻¹)	N° resolved peaks	FWHM (min); RSD (%)	μ_a (m ² ·V ⁻¹ ·s ⁻¹); RSD (%)	μ_e (m ² ·V ⁻¹ ·s ⁻¹); RSD (%)	N; RSD (%)
0.1	12	0.55 (RSD=0.59)	$6.55 \cdot 10^{-9}$ (RSD=0.76)	$5.85 \cdot 10^{-9}$ (RSD=0.85)	18385.82 (RSD=2.07)
0.5	11	0.65 (RSD=3.39)	$6.46 \cdot 10^{-9}$ (RSD=0.49)	$5.76 \cdot 10^{-9}$ (RSD=0.55)	13458.72 (RSD=7.74)
1	9	0.68 (RSD=0.39)	$6.62 \cdot 10^{-9}$ (RSD=0.28)	$5.91 \cdot 10^{-9}$ (RSD=0.31)	11650.84 (RSD=1.23)
2	10	0.82 (RSD=1.79)	$6.20 \cdot 10^{-9}$ (RSD=0.97)	$5.49 \cdot 10^{-9}$ (RSD=1.10)	8920.83 (RSD=3.52)
5	8	1.29 (RSD=2.80)	$6.12 \cdot 10^{-9}$ (RSD=1.27)	$5.41 \cdot 10^{-9}$ (RSD=1.43)	3794.70 (RSD=3.06)

S-VI Comparison with established EACA-based CZE-UV method

A comparison of the developed method and the EACA method developed by He *et al.* (2011) was made [9]. The relative abundances of the charge variants with their standard deviations measured with EACA and the MS-compatible method are represented in Table S4. The electropherograms measured under both conditions are shown in Fig. S10.

Table S4: Comparison of relative peak area percentage (%) of the total basic variants (B), main isoform (M), and acidic variants (A) from four mAbs (rituximab, NISTmAb, pembrolizumab, and cetuximab) (n=3) measured with EACA method and MS-compatible method. All the values are in percentage.

	EACA method			MS-compatible method		
	B (%)	M (%)	A (%)	B (%)	M (%)	A (%)
Rituximab	10.64 ± 2.81	79.29 ± 1.79	10.07 ± 2.28	10.04 ± 2.90	70.32 ± 0.40	19.65 ± 0.29
NISTmAb	31.48 ± 2.87	62.10 ± 1.16	6.42 ± 10.96	28.74 ± 0.33	68.06 ± 0.48	5.20 ± 7.73
Pembrolizumab	14.52 ± 1.42	74.50 ± 1.08	10.98 ± 8.53	15.83 ± 1.32	72.82 ± 0.43	11.35 ± 1.03
Cetuximab	11.65 ± 12.48	32.30 ± 4.00	56.04 ± 5.35	14.27 ± 7.27	29.06 ± 2.25	56.67 ± 0.72

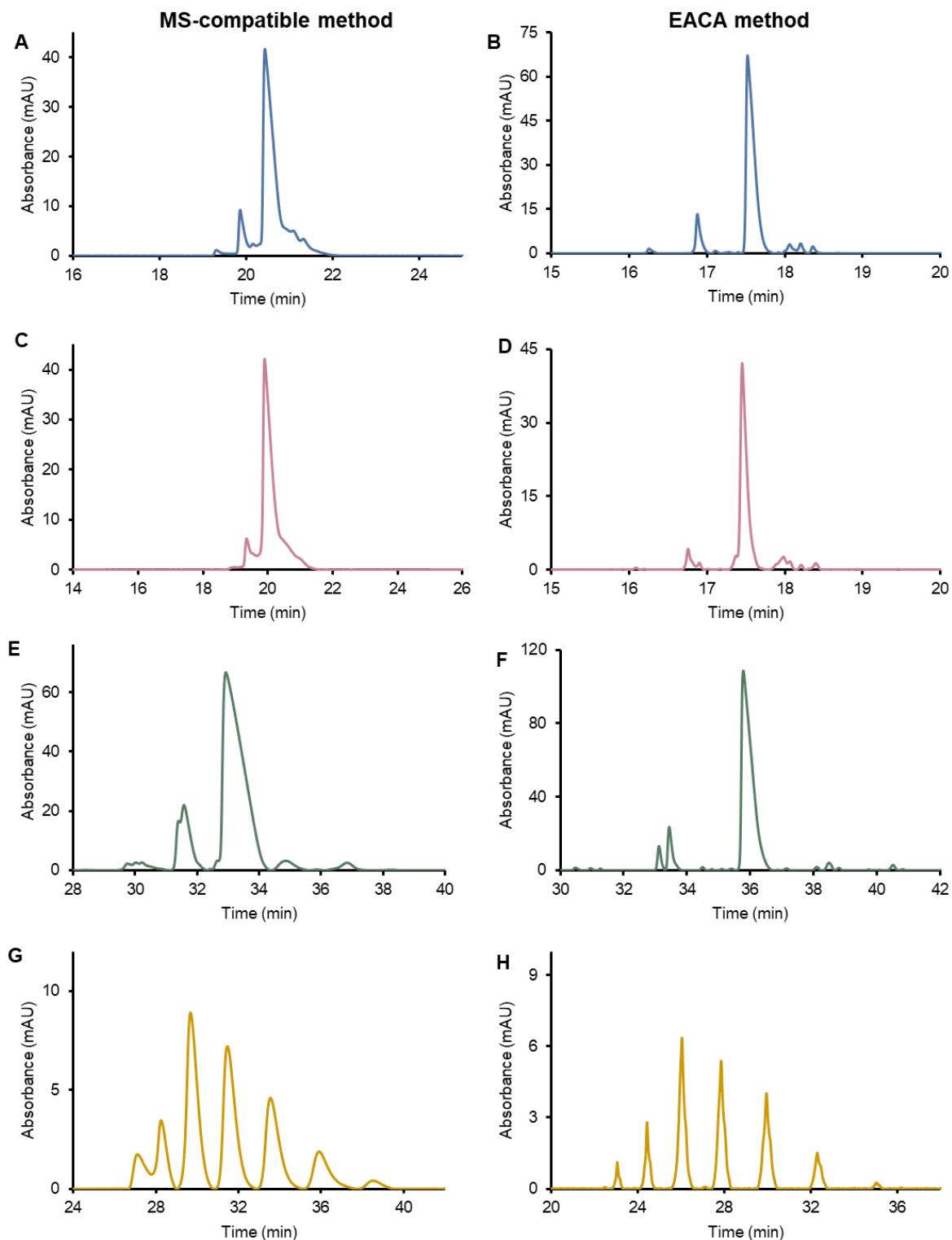


Fig. S10: CZE-UV of NISTmAb (**A and B**), rituximab (**C and D**), pembrolizumab (**E and F**), and cetuximab (**G and H**) measured with MS-compatible method (**A, C, E, G**) and the conditions of He *et al.* and Wiesner *et al.* (**B, D, F, H**). See sections 2.4.1 and 2.4.3 for additional information.

S-VII Optimization CZE-MS method

For the optimization of the MS parameters, pembrolizumab was used and infused into the MS at 10 $\mu\text{L}\cdot\text{min}^{-1}$ using a syringe pump. Table S5 shows the MS parameters used for this direct-infusion experiment. The isCID and S-lens RF levels were optimized between 50-100 eV and 50-100, respectively. The highest signal-to-noise ratio was obtained with 80 eV as isCID and 100 as S-lens RF level.

Table S5: MS settings for direct-infusion experiment with pembrolizumab

Parameter	Value
Voltage	3,500 V (positive polarity)
Capillary temperature	300 °C
Sheath gas	10 Arb
Microscans	10 ms
Scan range	1,500-6,000 m/z
Resolution	17,000

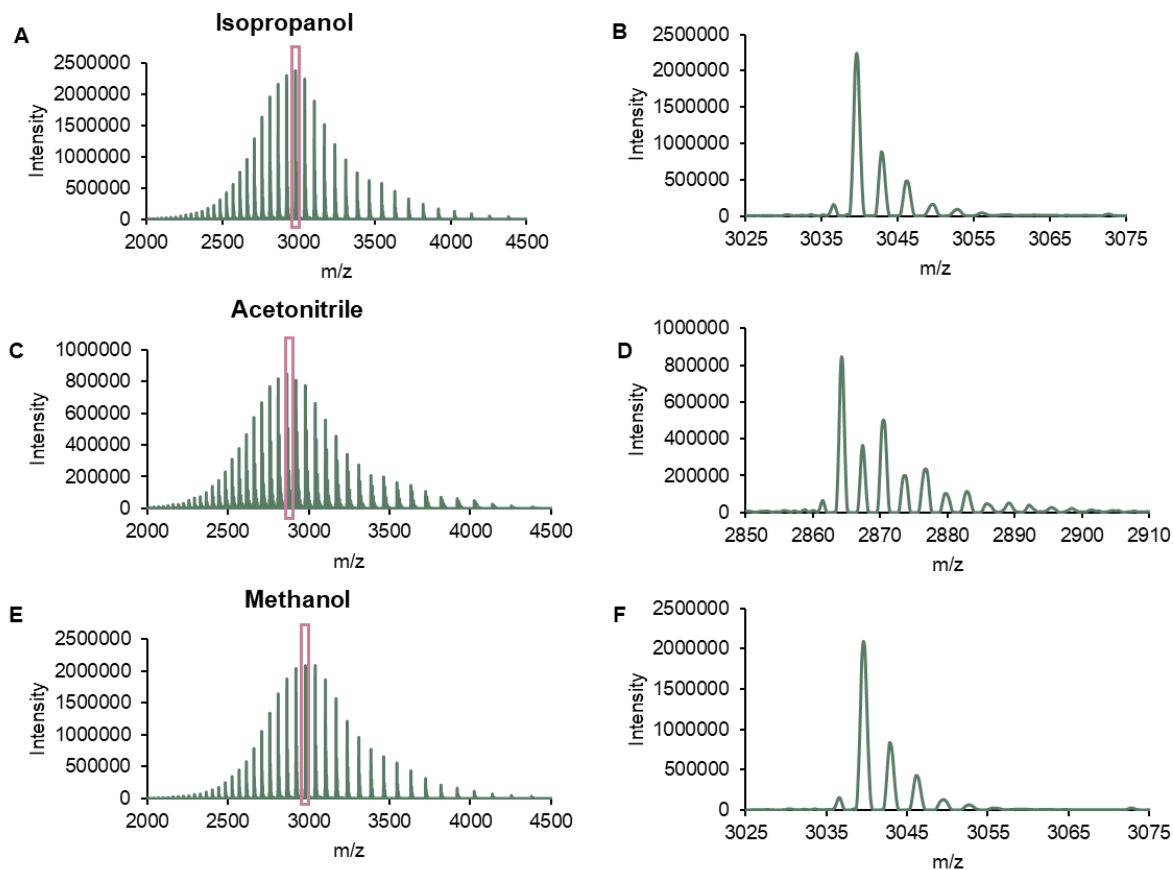


Fig. S11: Effect of sheath liquid composition on the charge state distribution of pembrolizumab ($1 \text{ mg} \cdot \text{mL}^{-1}$): **(A)** 0.5% (v/v) formic acid in 50/50 isopropanol/water, **(B)** zoom-in on charge state distribution measured with condition (A), **(C)** 0.5% (v/v) formic acid in 50/50 acetonitrile/water, **(D)** zoom-in on charge state distribution measured with condition (C), **(E)** 0.5% (v/v) formic acid in 50/50 methanol/water, **(F)** zoom-in on charge state distribution measured with condition (E). It should be noted that these measurements were measured with Orbitrap Fusion Lumos (Thermo Fisher Scientific, Bremen, Germany) which is limited in measuring until 4500 m/z. Therefore the charge state distribution differs with the measurements done on the Q Exactive Plus (high mass range mode). With isopropanol and methanol in sheath liquid, the charge distributions were quite similar. With acetonitrile as an organic solvent in the sheath liquid compositions, the signal intensity was lower compared to methanol and isopropanol.

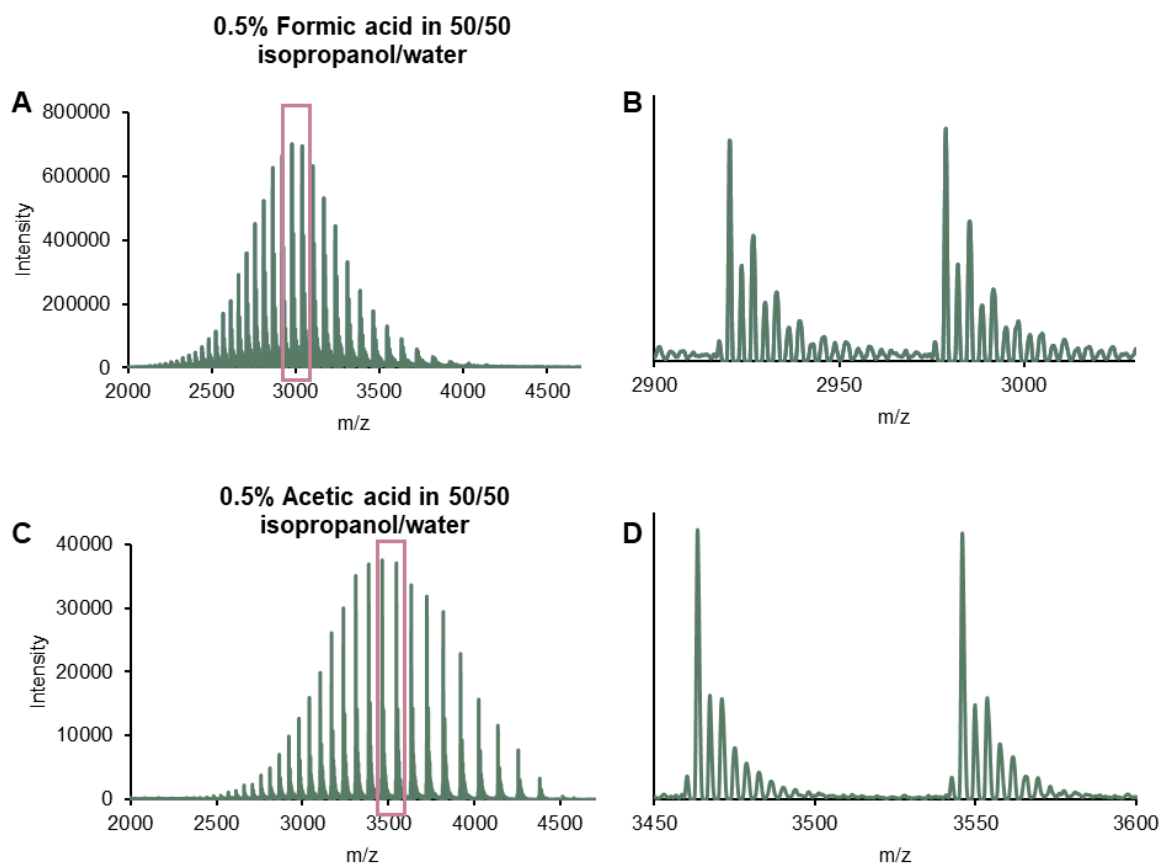


Fig. S12: Effect of acid type in sheath during CZE-MS of pembrolizumab ($1 \text{ mg}\cdot\text{mL}^{-1}$): **(A)** 0.5% (v/v) formic acid in 50/50 isopropanol/water, **(B)** zoom-in on charge state distribution measured with condition (A), **(C)** 0.5% (v/v) acetic acid in 50/50 isopropanol/water, **(D)** zoom-in on charge state distribution measured with condition (C). There is a shifted charge state distribution with 0.5% (v/v) acetic acid in 50/50 water/isopropanol compared to 0.5% (v/v) formic acid in 50/50 water/isopropanol.

0.5% (v/v) Acetic acid in 50/50 isopropanol/water

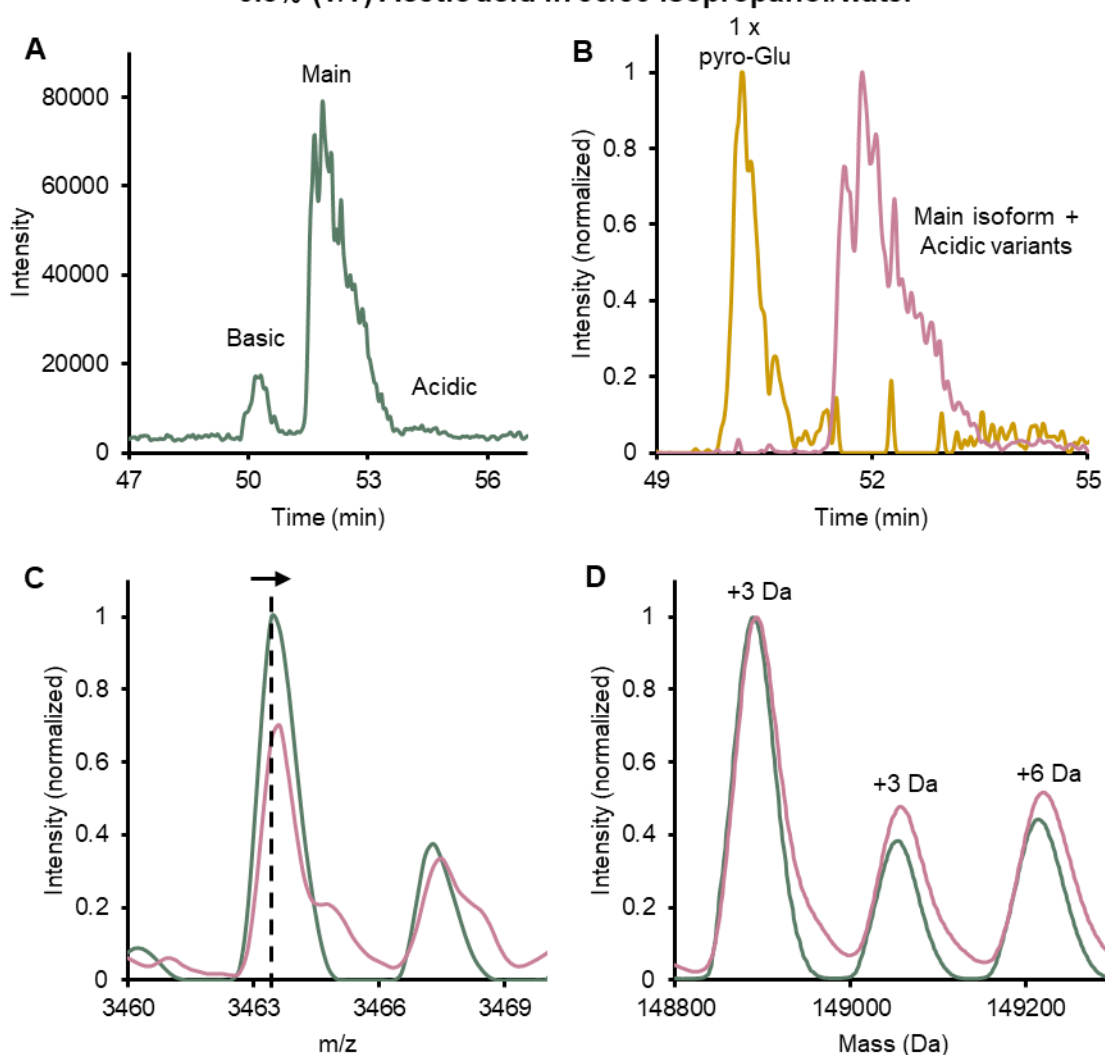


Fig. S13: Effect of 0.5% (v/v) acetic acid in 50/50 isopropanol/water in sheath liquid on CZE-MS of pembrolizumab ($1 \text{ mg} \cdot \text{mL}^{-1}$): **(A)** BPE, **(B)** EIE of basic variants (yellow) and main isoform + acidic variants (pink). Conversion of N-terminal pyroglutamate is assigned as pyro-Glu. **(C)** Zoom in on the charge state distribution of the main isoform (green) and acidic variants (pink). There is a small shift visible, meaning that possible acidic variants (higher m/z) are separated from the main isoform (lower m/z), **(D)** Deconvoluted spectrum of the main isoform (green), and acidic variants (pink). The difference in masses is indicated above the peak. Conditions: HPMC-coated capillary ($50 \mu\text{m}$ i.d. \times 70 cm), BGE 50 mM acetic acid (pH 5.0), separation voltage $+20 \text{ kV}$. For 0.5% (v/v) formic acid in 50/50 isopropanol/water. Note that there is a difference in migration time (Figs. S13 and S14) due to the capillary difference and different velocities at the end of the capillary (difference in counterion in sheath liquid). The one-time conversion to N-terminal pyroglutamate (pyro-Glu) (basic variants) could not be separated from the main isoform. The acidic variants are not resolved from the main variant. However, there is a small shift in m/z which could be an indication of deamidation.

0.5% (v/v) Formic acid in 50/50 isopropanol/water

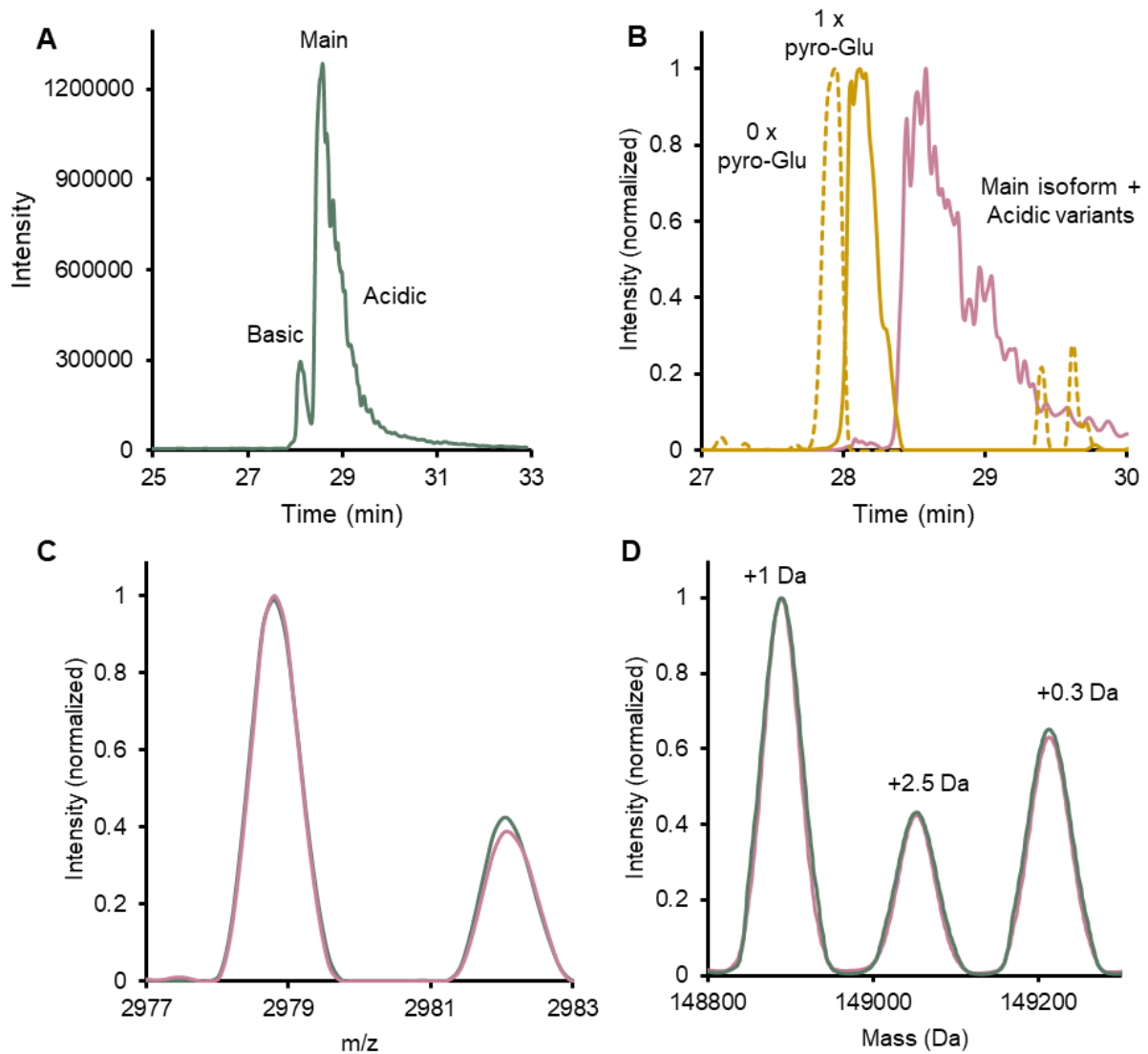


Fig. S14: Effect of 0.5% (v/v) formic acid in 50/50 isopropanol/water in sheath liquid on CZE-MS of pembrolizumab ($1 \text{ mg} \cdot \text{mL}^{-1}$): **(A)** BPE, **(B)** EIE of basic variants (yellow, dashed and solid) and main isoform + acidic variants (pink, solid). Conversion of N-terminal pyroglutamate is assigned as pyro-Glu. **(C)** Zoom in on the charge state distribution of the main isoform (green) and acidic variants (pink). There is a small shift visible, meaning that possible acidic variants (higher m/z) are separated from the main isoform (lower m/z), **(D)** Deconvoluted spectrum of the main isoform (green), and acidic variants (pink). The difference in masses is indicated above the peak. Conditions: HPMC-coated capillary (50 μm i.d. x 60 cm), BGE 50 mM Acetic acid (pH 5.0), separation voltage +20 kV. For 0.5% (v/v) formic acid in 50/50 isopropanol/water. Note that the zero and one-time conversion to N-terminal pyroglutamate (basic variants) could be identified from the main isoform.

S-VIII Profiling of mAbs by CZE-MS

The extracted ion electropherograms (EIE) are depicted for NISTmAb, rituximab, cetuximab, and pembrolizumab.

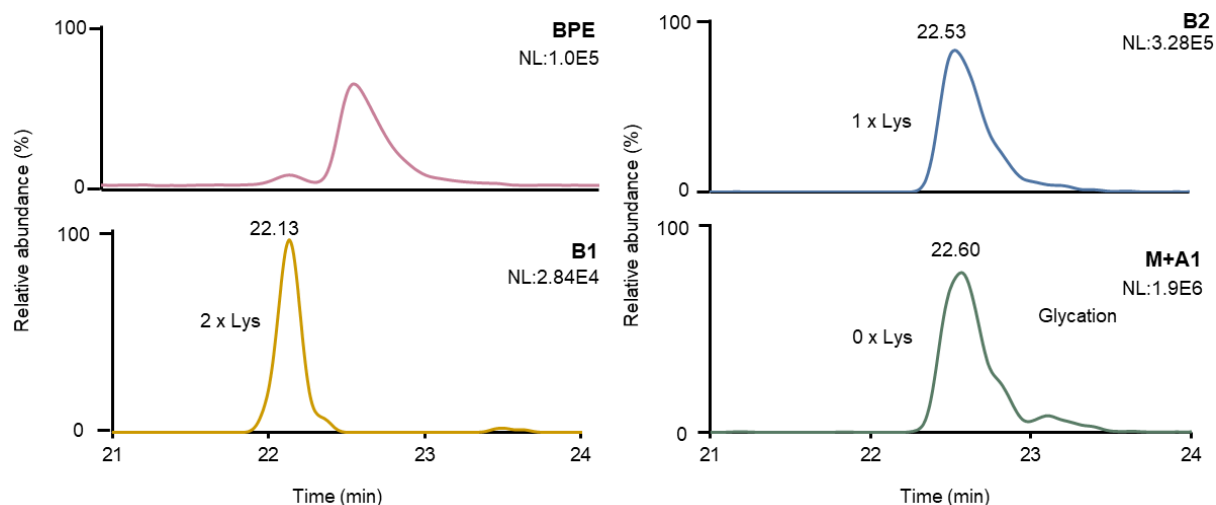


Fig. S15: CZE-MS of NISTmAb. The BPE and the EIEs of the basic variants (B1 and B2) main isoform (M, and acidic variants (A1) are plotted. The presence of C-terminal lysine is indicated with Lys. The EIEs were created based on the m/z values in Table S6. Conditions: HPMC-coated capillary (50 μm i.d. x 60 cm), BGE 50 mM acetic acid (pH 5.0), separation voltage +20 kV, sheath liquid 0.5% (v/v) formic acid in 50/50 isopropanol/water. See sections 2.4.1 and 2.4.2 for detailed CE and MS settings.

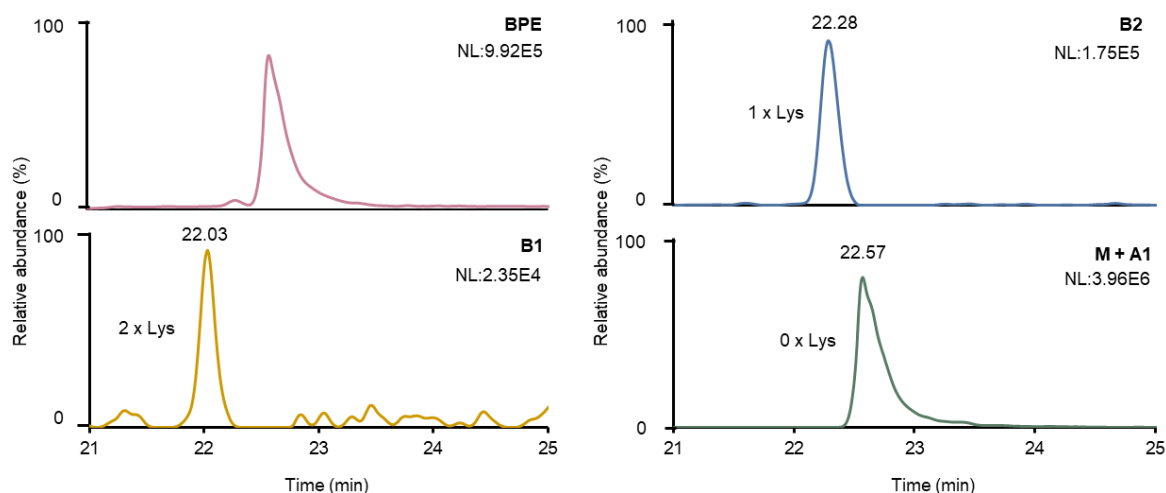


Fig. S16: CZE-MS of rituximab. The BPE and the EIEs of the basic variants (B1 and B2), main isoform (M) and acidic variants (A1) are plotted. The presence of C-terminal lysine is indicated with Lys. The EIEs were created based on the m/z values in Table S6. Conditions: HPMC-coated capillary (50 μm i.d. x 60 cm), BGE 50 mM acetic acid (pH 5.0), separation voltage +20 kV, sheath liquid 0.5% (v/v) formic acid in 50/50 isopropanol/water. See sections 2.4.1 and 2.4.2 for detailed CE and MS settings.

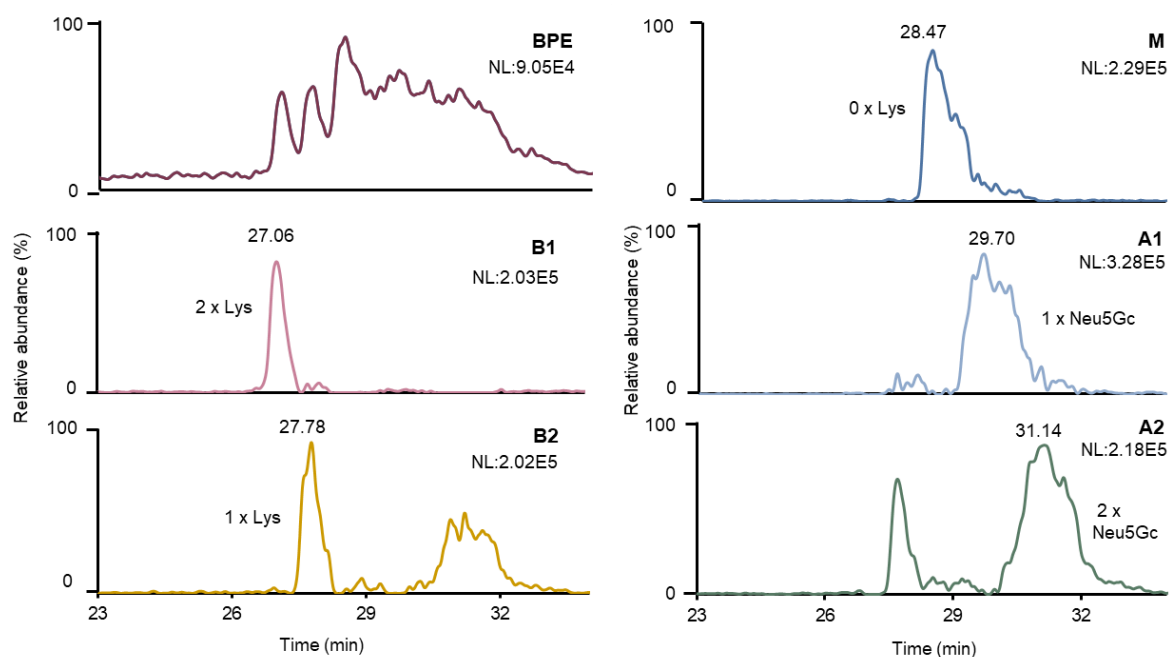


Fig. S17: CZE-MS of cetuximab. The BPE and the EIEs of the basic variants (B1 and B2), main isoform (M), and acidic variants (A1 and A2) are plotted. The C-terminal lysine is indicated with Lys whereas sialylated glycoforms are indicated with Neu5Gc. The EIEs were created based on the m/z values in Table S6. Conditions: HPMC-coated capillary (50 μm i.d. x 60 cm), BGE 50 mM acetic acid (pH 5.0), separation voltage +20 kV, sheath liquid 0.5% (v/v) formic acid in 50/50 isopropanol/water. See sections 2.4.1 and 2.4.2 for detailed CE and MS settings. Note that due to the heterogeneity of cetuximab, multiple charge variants are present. For B2 and A2, there is an extra peak visible due to the overlap in m/z ratios.

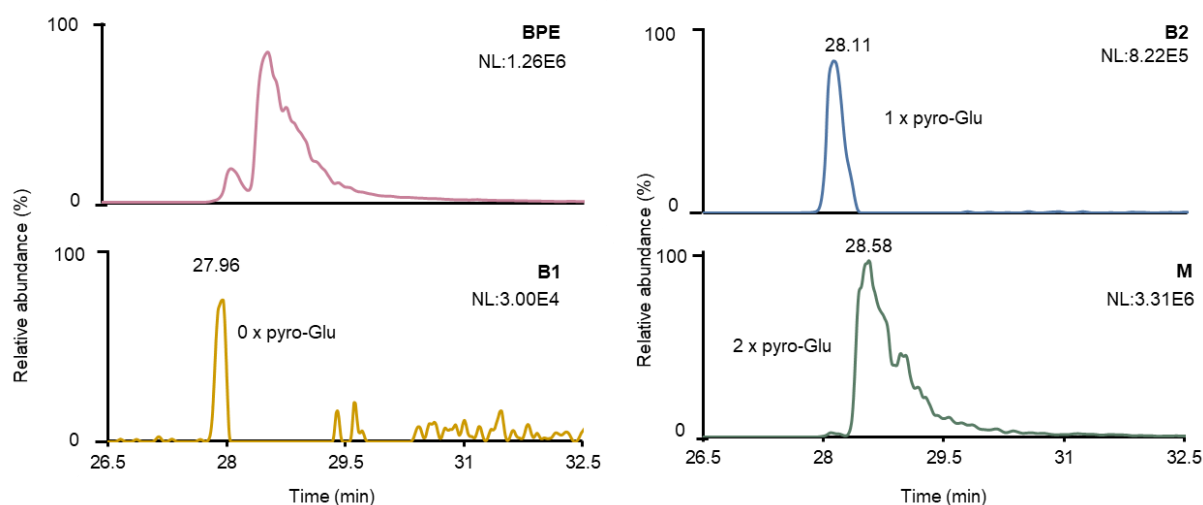


Fig. S18: CZE-MS of pembrolizumab. The BPE and the EIEs of the basic variants (B1 and B2) and main isoform (M) are plotted. Conversion to N-terminal pyroglutamate is indicated with pyro-Glu. The EIEs were created based on the m/z values in Table S6. Conditions: HPMC-coated capillary (50 μm i.d. x 60 cm), BGE 50 mM acetic acid (pH 5.0), separation voltage +20 kV, sheath liquid 0.5% (v/v) formic acid in 50/50 isopropanol/water. See sections 2.4.1 and 2.4.2 for detailed CE and MS settings.

Table S6: The m/z values for the generation of the EIEs of the four analyzed antibodies (NISTmAb, pembrolizumab, rituximab, and cetuximab). The peaks of the charge variants are indicated with (i) B, basic variants, (ii) M, main isoform, (iii), A, acidic variants. A Gaussian smoothing parameter of 11 was applied for the generation of the EIEs. The mass tolerance was set to 0.50 amu.

	B1 (m/z)	B2 (m/z)	M (m/z)	A1 (m/z)	A2 (m/z)
NISTmAb	4014.2-4014.6, 4212.3-4212.6, 4239.0-4239.3, 4363.6-4363.9, 3908.6-3908.9	4006.4-4006.7, 4117.7-4118.0, 4235.3-4235.6, 4359.9-4360.2, 4496.8-4497.1	3901.0-3901.4, 4006.6-4006.9, 4117.7-4118.0, 4235.4-4235.7, 4360.0-4360.3*		
Pembrolizumab	2865.0-2865.3, 2921.1-2921.4, 2979.6-2979.9, 3040.3-3040.7	2864.6-2864.9, 2920.7-2921.0, 2979.1-2979.3, 3039.9-3040.2, 3103.2-3103.5	2864.2-2864.5, 2920.3-2920.6, 2978.8-2979.0, 3039.5-3039.7, 3102.9-3103.2*		
Rituximab	3348.4-3348.7, 3426.2-3426.5, 3507.8-3508.1, 3589.3-3589.6, 3675.1-3675.4, 3773.3-3773.7	3346.0-3346.3, 3427.6-3427.9, 3505.3-3505.6, 3590.8-3591.1, 3680.5-3680.8, 3779.0-3779.3	3347.3-3347.6, 3428.9-3429.2, 3510.5-3510.8, 3592.1-3592.4, 3681.9-3682.2, 3776.3-3776.6*		
Cetuximab	3251.4-3251.7, 3322.1-3322.4, 3395.8-3396.1, 3473.0-3473.3, 3553.8-3554.1, 3638.4-3638.7, 3642.3-3642.6	3248.7-3249.0, 3319.3-3319.6, 3393.0-3393.3, 3470.1-3470.4, 3350.8-3351.1, 3635.3-3635.6	3246.0-3246.3, 3316.5-3316.8, 3390.2-3390.5, 3467.2-3467.5, 3547.8-3548.1, 3632.3-3632.5	3249.1-3249.3, 3319.7-3320.0, 3393.4-3393.7, 3470.5-3470.8, 3551.2-3551.5, 3635.8-3636.1	3252.1-3252.4, 3322.9-3323.2, 3396.7-3397.0, 3473.8-3474.1, 3554.6-3554.9, 3639.2-3639.5, 3728.1-3728.4, 3821.3-3821.6

*As the acidic variants were not fully resolved from the main isoform for NISTmAb, pembrolizumab, and rituximab, the m/z values of EIE of the main variant may also contain acidic variants species.

Table S7: Deconvoluted masses (in Da) of the main isoform and basic and acidic variants of NISTmAb, pembrolizumab, rituximab, and cetuximab. The mass error is represented in Da. The N-glycoforms are assigned as reported here [10], C-terminal lysine residual is indicated as Lys, N-terminal pyroglutamate formation as pyro-Glu, and oxidation as Ox.

	Theoretical mass (Da)	Experimental mass (Da)	Mass error (Da)	
NISTmAb				
G0/G0F	147,833.9	147,838.5	4.6	
G0F/G1F	148,199.2	148,203.5	4.3	
G1F/G1F or G0F/G2F	148,361.4	148,364.0	2.6	
G1F/G2F	148,523.5	148,524.7	1.2	
G2F/G2F	148,685.6	148,687.4	1.8	
G0F/G0F + 1 Lys	148,165.3	148,169.7	4.4	
G0F/G1F + 1 Lys	148,327.4	148,330.0	2.6	
G1F/G1F + 1 Lys	148,489.6	148,491.0	1.4	
G1F/G2F + 1 Lys	148,651.7	148,652.3	0.6	
G2F/G2F + 1 Lys	148,976.0	148,980.3	4.3	
G0F/G1F + 2 Lys	148,455.6	148,461.5	5.9	
G1F/G1F + 2 Lys	148,617.8	148,623.9	6.1	
Pembrolizumab				
G0/G0F	148,741.8	148,745.0	3.2	
G0F/G0F	148,888.0	148,890.3	2.3	
G0F/G1F	149,050.1	149,053.3	3.2	
G1F/G1F	149,212.3	149,212.9	0.6	
G1F/G2F	149,374.4	149,378.2	3.8	
G2F/G2F	149,536.5	149,536.0	-0.5	
G0F/G0F + 0 x pyro-Glu	149,083.0	149,094.8	8.0	
G1F/G1F + 0 x pyro-Glu	149,245.1	149,248.6	3.5	
G1F/G2F + 0 x pyro-Glu	149,407.3	149,414.9	7.6	
G2F/G2F + 0 x pyro-Glu	149,569.4	149,573.2	3.8	
G0/G0F + 1 x pyro-Glu	148,758.6	148,759.3	0.4	
G0F/G0F + 1 x pyro-Glu	148,905.0	148,907.0	2.0	
G0F/G1F + 1 x pyro-Glu	149,067.1	149,071.4	4.3	
G1F/G1F + 1 x pyro-Glu	149,229.3	149,229.8	0.5	
G1F/G2F + 1 x pyro-Glu	149,391.4	149,392.4	1.0	
G2F/G2F + 1 x pyro-Glu	149,553.6	149,552.3	-1.3	
Rituximab*				
G0F/G0F	147,074.0	147,079.4	5.4	
G0F/G1F	147,238.2	147,240.8	2.6	
G1F/G1F or G0F/G2F	147,400.3	147,403.0	2.7	
G1F/G2F	147,562.4	147,565.9	3.5	
G2F/G2F	147,724.6	147,728.6	4.0	
G0F/G0F + 2 Lys + 1 Ox	147,348.4	147,345.7	-2.7	
G0F/G1F + 2 Lys + 1 Ox	147,510.5	147,510.2	-0.3	
G1F/G1F or G0F/G2F + 2 Lys + 1 Ox	147,672.6	147,670.2	-2.4	
G1F/G2F + 2 Lys + 1 Ox	147,834.8	147,835.0	0.2	
G2F/G2F + 2 Lys + 1 Ox	147,996.9	147,991.5	-5.4	
G1F/G1F or G0F/G2F + 1 Lys + 2 Ox	147,560.5	147,567.1	6.6	
G2F/G2F + 1 Lys + 2 Ox	147,884.8	147,890.9	6.1	
Cetuximab**				
H7N4F1/H7N4F1	M5/G0F	152,123.4	152,128.2	4.8
	G0F/G0F	152,351.7	152,354.3	2.6
	G0F/G1F	152,513.8	152,516.3	2.5
	G1F/G1F	152,676.0	152,677.9	1.9
	M5/G0F + 2 Lys	152,379.7	152,383.1	3.4
	G0F/G0F + 2 Lys	152,608.0	152,611.6	3.6
	G0F/G1F + 2 Lys	152,769.8	152,771.9	2.1
	G1F/G1F + 2 Lys	152,932.3	152,934.7	2.4
	M5/G0F + 1 Lys	152,251.6	152,256.0	4.4
	G0F/G0F + 1 Lys	152,479.9	152,483.0	3.1
	G0F/G1F + 1 Lys	152,641.6	152,643.9	2.3
	G1F/G1F + 1 Lys	152,804.2	152,807.3	3.1
	M5/G1F	152,123.4	152,128.2	4.8

H7N4F1/H6N4F1	G0F/G0F	152,189.6	152,192.4	2.8
	G0F/G1F	152,351.7	152,354.3	2.6
	G1F/G1F	152,513.8	152,516.3	2.5
	M5/G1F + 2 Lys	152,379.7	152,383.1	3.4
	G0F/G1F + 2 Lys	152,608.0	152,611.6	3.6
	G1F/G1F + 2 Lys	152,769.8	152,771.9	2.1
	M5/G1F + 1 Lys	152,251.6	152,256.0	4.4
	G1F/G1F + 1 Lys	152,641.6	152,643.9	2.3
H6N4F1/H6N4F1	G0F/G0F	152,027.4	152,029.0	1.6
	G0F/G1F	152,189.6	152,192.4	2.8
	G1F/G1F	152,351.7	152,354.3	2.6
	G0F/G0F + 2 Lys	152,283.7	152,290.8	7.0
	G1F/G1F + 2 Lys	152,608.0	152,611.6	3.6
	G0F/G0F + 1 Lys	152,155.6	152,163.5	8.0
	G0F/G1F + 1 Lys	152,317.8	152,325.9	8.1
	G1F/G1F + 1 Lys	152,479.9	152,483.0	3.1
H7N4F1/H6N4F1S1	G0F/G0F	152,496.8	152,501.9	5.1
	G0F/G1F	152,658.9	152,662.3	3.4
	G1F/G1F	152,821.1	152,824.0	2.9
H6N4F1S1/H6N4F1	G0F/G0F	152,334.7	152,344.7	10.0
	G0F/G1F	152,496.8	152,501.9	5.1
	G1F/G1F	152,658.9	152,662.3	3.4
H6N4F1S1/H6N4F1S1	G0F/G0F	152,641.9	152,648.6	6.7
	G0F/G1F	152,804.1	152,808.3	4.2
	G1F/G1F	152,966.2	152,967.6	1.4

*For Rituximab, the theoretical masses were calculated based on these studies.[2,11]

**Due to the four glycosylation sites of cetuximab, the N-glycoforms of the Fc and Fab regions are represented in the table. The N-glycoforms in the Fab region are assigned as; H7N4F1/H7N4F1, H7N4F1H6N4F1S1, H7N4F1/H6N4F1, H6N4F1/H6N4F1S1, H6N4F1/H6N4F1. H is Hexose, N is N-Acetylglucosamine, F is fucose and S is N-Glycolylneuraminic acid. The theoretical masses are used from the study of Lippold *et al.*[10]

Table S8: Deconvoluted masses (in Da) of the main isoform and acidic variant of pembrolizumab. It was measured at 35,000 resolution. Delta mass was calculated between the measured mass of the main isoform and acidic variant in Da. The glycoforms are assigned as reported here [10], N-terminal pyroglutamate formation as pyro-Glu, and deamidation of isoaspartic acid or aspartic acid as Asp.

	Main isoform (Da)	Acidic variant (Da)	Delta mass (Da)
G0/G0F + 2 x pyro-Glu + Asp	148,743.3	148,744.4	1.1
G0F/G0F + 2 x pyro-Glu + Asp	148,888.5	148,889.7	1.2
G0F/G1F + 2 x pyro-Glu + Asp	149,050.6	149,053.1	2.4
G1F/G1F + 2 x pyro-Glu + Asp	149,212.2	149,211.9	0.3
G1F/G2F + 2 x pyro-Glu + Asp	149,376.9	149,378.1	1.2
G2F/G2F + 2 x pyro-Glu + Asp	149,535.0	149,537.6	2.6

References

- [1] Goyon A, Excoffier M, Janin-Bussat M-C, Bobaly B, Fekete S, Guillarme D, et al. Determination of isoelectric points and relative charge variants of 23 therapeutic monoclonal antibodies. *Journal of Chromatography B* 2017;1065–1066:119–28. <https://doi.org/10.1016/j.jchromb.2017.09.033>.
- [2] Di Marco F, Berger T, Esser-Skala W, Rapp E, Regl C, Huber CG. Simultaneous Monitoring of Monoclonal Antibody Variants by Strong Cation-Exchange Chromatography Hyphenated to Mass Spectrometry to Assess Quality Attributes of Rituximab-Based Biotherapeutics. *Int J Mol Sci* 2021;22:9072. <https://doi.org/10.3390/ijms22169072>.
- [3] Turner A, Schiel JE. Qualification of NISTmAb charge heterogeneity control assays. *Anal Bioanal Chem* 2018;410:2079–93. <https://doi.org/10.1007/s00216-017-0816-6>.
- [4] Füssl F, Trappe A, Carillo S, Jakes C, Bones J. Comparative Elucidation of Cetuximab Heterogeneity on the Intact Protein Level by Cation Exchange Chromatography and Capillary Electrophoresis Coupled to Mass Spectrometry. *Anal Chem* 2020;92:5431–8. <https://doi.org/10.1021/acs.analchem.0c00185>.
- [5] Shah B, Zhu Y, Wypych J, Zhang Z. Observation of Heavy-Chain C-Terminal Des-GK Truncation in Recombinant and Human Endogenous IgG4. *J Pharm Sci* 2023;112:1845–9. <https://doi.org/10.1016/j.xphs.2023.05.005>.
- [6] Zhang X, Kwok T, Zhou M, Du M, Li V, Bo T, et al. Imaged capillary isoelectric focusing (icIEF) tandem high resolution mass spectrometry for charged heterogeneity of protein drugs in biopharmaceutical discovery. *J Pharm Biomed Anal* 2023;224:115178. <https://doi.org/10.1016/j.jpba.2022.115178>.
- [7] Desai MJ, Armstrong DW. Separation, Identification, and Characterization of Microorganisms by Capillary Electrophoresis. *Microbiology and Molecular Biology Reviews* 2003;67:38–51. <https://doi.org/10.1128/MMBR.67.1.38-51.2003>.
- [8] Beckers JL, Everaerts FM, Ackermans MT. Determination of absolute mobilities, pK values and separation numbers by capillary zone electrophoresis. *J Chromatogr A* 1991;537:407–28. [https://doi.org/10.1016/S0021-9673\(01\)88914-7](https://doi.org/10.1016/S0021-9673(01)88914-7).
- [9] He Y, Isele C, Hou W, Ruesch M. Rapid analysis of charge variants of monoclonal antibodies with capillary zone electrophoresis in dynamically coated fused-silica capillary. *J Sep Sci* 2011;34:548–55. <https://doi.org/10.1002/jssc.201000719>.
- [10] Lippold S, Nicolardi S, Wuhrer M, Falck D. Proteoform-Resolved Fc γ R1IIa Binding Assay for Fab Glycosylated Monoclonal Antibodies Achieved by Affinity Chromatography Mass Spectrometry of Fc Moieties. *Front Chem* 2019;7. <https://doi.org/10.3389/fchem.2019.00698>.
- [11] Samonig M, Huber C, Scheffler K. LC/MS Analysis of the Monoclonal Antibody Rituximab Using the Q Exactive Benchtop Orbitrap Mass Spectrometer 2016. <https://doi.org/10.13140/RG.2.1.4538.9846>.